

Analytical Approach for the Power Management of Blended-Mode Plug-In Hybrid Electric Vehicles

Menyang Zhang, *Member, IEEE*, Yan Yang, and Chunting Chris Mi, *Fellow, IEEE*

Abstract—This paper focuses on the intrinsic aspects of power management for hybrid electric vehicles (HEVs) and plug-in HEVs (PHEV). A vehicle power distribution density function is used to describe the drive cycle characteristics. An electric driveline loss is introduced to describe the minimum system loss for a given mechanical power output, and a piecewise linear fuel consumption model is used to capture essential characteristics such as idle fuel consumption rate, peak efficiency, and the minimum power to reach peak efficiency. Models are based on the assumption that both machines operate at the optimal speed and torque for a given mechanical power as if they are coupled with an ideal continuous variable transmission (CVT). The power management strategy is represented with a pair of power parameters that describe the power threshold for turning on the engine and the optimum battery power in engine-on operations. The model of a parallel hybrid electric powertrain is constructed to obtain optimal solutions that maximize the fuel economy for a given battery energy depletion and for a general vehicle power distribution density function. One-dimensional loss models of two power sources as approximations to real machines coupled with hypothetical CVTs are introduced to solve the optimization problem analytically. It is found that the optimal minimum engine power is the controlling factor in minimizing the total fuel consumption for the given battery energy depletion targets and that the optimal power is solely determined by powertrain characteristics. Numerical simulations validated the properties of the optimal power solutions obtained through analytic approaches. The significance of the results to real-world HEV and PHEV applications are also discussed.

Index Terms—Analytical method, blended plug-in hybrid electric vehicles (PHEV), electric vehicle, parallel hybrid, plug-in HEV (PHEV), power management.

I. INTRODUCTION

HYBRID and plug-in hybrid electric vehicles (HEV/PHEV) have become promising in the automotive world because of their low fuel consumption and low emissions. The inclusion of the secondary power source

(battery and electric motor) leads to the benefits of improved fuel efficiency and reduced emissions [1]–[5]. The propulsion power in HEV/PHEV comes from two drive trains: 1) the electric drive train and 2) the internal combustion engine (ICE) drive train. The general problem in HEV/PHEV propulsion system design is how to optimize the power split between the battery and the engine to minimize fuel consumption and emissions while maintaining good driving performance [6]–[11].

PHEVs use grid electricity to power the vehicle for an initial driving range, referred to as charge depletion (CD) mode. Using electric energy from the utility grid to displace part of the fuel is the major feature of PHEVs [12]–[23]. There are two basic types of PHEV: 1) extended range electric vehicles (EREVs) and 2) blended-mode PHEVs.

EREVs offer pure electric driving capability in the initial driving range, referred to as all-electric range (AER). To realize pure electric driving in all driving conditions, EREVs are equipped with a full-sized traction motor powered by the battery pack. One of the disadvantages of EREVs is the increased system cost due to the full-sized traction motor and power requirements for the battery; the other is the high losses in the electric system (battery and electric motor) at high power operations. These constraints have led to the concept of blended-mode PHEV.

A blended-mode PHEV usually has less electric drive capability. Therefore, it can typically achieve cruise and moderate acceleration in the electric mode at low to moderate vehicle speeds. For operations requiring either higher power or higher torque, the thermal engine must be used either with or without electric assistance, depending on vehicle control strategies. The blended operation can also be adopted by EREVs to reduce system losses at higher power demands.

One of the PHEV's primary capabilities is fuel displacement by depleting the onboard electric energy storage system (ESS) to a preset low-threshold state of charge (SOC). It is generally desirable that the onboard ESS has reached this depleted state (charge sustaining SOC) by the end of the "designed" vehicle travel distance. On one hand, aggressive CD may result in a higher electric loss incurred in the vehicle system and affect the overall energy efficiency of the vehicle, i.e., more energy is consumed whether it is from gasoline or electricity. On the other hand, vehicles with less than sufficient charge-depleting operations may not achieve fuel displacement function as designed, and the capacity of the onboard ESS is underutilized. Therefore, how to achieve optimized CD operations in PHEV applications is one of the fundamental problems of PHEV control.

Manuscript received April 13, 2011; revised August 12, 2011, October 18, 2011, and November 28, 2011; accepted January 26, 2012. Date of publication February 10, 2012; date of current version May 9, 2012. This work was supported in part by the U.S. Department of Energy and in part by the Chrysler Group, LLC. The review of this paper was coordinated by Prof. L. Guvenc.

M. Zhang is with the Chrysler Group, LLC, Auburn Hills, MI 48326 USA (e-mail: mz91@chrysler.com).

Y. Yang was with the Department of Electrical and Computer Engineering, University of Michigan, Dearborn, MI 48128 USA. She is now with Cummins Inc., Columbus, IN 47202-3005 USA (e-mail: yangyan801230@gmail.com).

C. C. Mi is with the Department of Electrical and Computer Engineering, University of Michigan, Dearborn, MI 48128 USA (e-mail: chrismi@umich.edu).

Color versions of one or more of the figures in this paper are available online at <http://ieeexplore.ieee.org>.

Digital Object Identifier 10.1109/TVT.2012.2187318

Control strategies for a blended-mode PHEV can be complex and multidimensional and will have significant impact on vehicle performance, drivability, and fuel consumption [24]–[31]. In [24], a comparison between AER strategy and blended mode CD strategy were investigated, and it was concluded that the proposed blended mode strategy can improve a PHEV's fuel economy by up to 9% for a power-split configuration. Most of the gain is from operating the engine more efficiently. However, detailed control algorithm, such as engine on–off threshold, was not explicitly given. In [25] and [26], stochastic dynamic programming was used to develop a supervisory control strategy for a hybrid vehicle that coordinates the operation of vehicle subsystems to achieve performance targets such as maximizing fuel economy and reducing exhaust emissions. PHEV is not studied in this paper. In [27], an intelligent energy management system was developed to intelligently allocate power to the vehicle battery chargers through real-time monitoring and control to ensure optimal usage of available power, charging time, and grid stability. Vehicle operating efficiency is not one of the goals of this paper. In [28], a comparative analysis is presented of the fuel economy and the greenhouse gas emissions between a conventional HEV and the PHEV developed at the University of Technology, Sydney. A special energy management strategy was developed for the power management of the PHEV. The control is a rule-based strategy that controls the single onboard electric machine to operate either as a motor or as a generator. In [29], an energy storage management strategy is developed for the PHEV based on a heuristic and on a model predictive control scheme to realize the balancing functions for the power grid using PHEVs. In [30] and [31], the effects of different PHEV control strategies on the vehicle performance of HEV and PHEV are compared, and in [30], the focus is on conventional HEV with emphasis on developing control strategies based on intelligent systems approaches. In [31], an equivalent consumption minimization strategy was developed to control the PHEV in both EV and blended modes. The focus of these control strategies is primarily intelligent-system-based approaches. Due to the complexity and computation time needed in these control strategies, it is often hard to implement in real time for the vehicle control, although they seem feasible in simulations. It is also unclear whether an “optimal charge-depleting strategy” calibrated for a given drive cycle and a battery depletion target remains optimal for different drive cycles and battery depletion targets [32]–[38].

In an earlier paper published by two of the authors of this paper, a control strategy based on optimal power operations of the PHEV was developed [39]. Based on the proposed strategy, if the trip distance exceeds AER, the proposed optimal power strategy can perform better than the electric dominant control strategy. Only the total fuel consumption during specific drive cycles are considered based on the electric system loss characteristics, vehicle power demand, total battery energy, and trip distance. It does not rely on detailed trip information other than the total trip distance. Therefore, it is possible to implement the control strategy in real time if the total distance is known before the trip. Since most people commuting to work know their approximate driving distance, this control strategy can potentially provide significant fuel savings. While the focus

of that paper is on PHEV, and the engine on/off threshold was derived for the optimal power control strategy, the paper does not give a generalized solution for overall vehicle level fuel optimization, such as cycle characteristics, battery depletion targets, and powertrain characteristics.

Therefore, it is the motivation of the authors of this paper to provide the insights about how the optimal charge-depleting strategy is related to powertrain system characteristics, cycle characteristics, and battery energy depletion targets and to provide the basic properties of the optimal strategy that can be used for real-world applications. Simplified models that capture the very essences of the system are introduced for developing analytic solutions to the optimization problem, as defined in this paper. Hence, this paper focuses on the control parameter optimization for a parallel PHEV. The PHEV model is defined on the basis of ICE fuel consumption characteristics and electric power loss characteristics. The detailed mathematic analysis is employed to obtain the optimal solutions. The impacts of vehicle system properties, driving cycles, and battery energy depletion targets on the optimal strategy are evaluated through simulations. The general properties of the control strategy and their significance to parallel PHEVs and HEVs are discussed.

II. MODEL CONSTRUCTION

In this paper, a parallel ICE–electric powertrain architecture is defined as shown in Fig. 1. In this architecture, the propulsion power comes from two energy resources: 1) gasoline-based ICE and 2) electricity-based battery pack. A parallel gasoline–electric hybrid transmission is capable to transmit the desired ICE power and desired motor mechanical power to meet the vehicle driving power demand. When the engine output power exceeds the driving power demand, the excessive power will be used to recharge the battery through the electric driveline.

In this paper, the vehicle power demand is defined as the total required mechanical power P_o from the vehicle power plant without frictional braking. It includes the accessory power, driveline losses, and the wheel driving power needed for vehicle acceleration under vehicle road loads.

A. Electric Loss Model

As shown in Fig. 1, the battery power is the sum of the mechanical power output from the electrical motor and the total power losses of the battery, converter, and electric motor. Among these losses, battery loss is more significant at high discharge power. The electric losses in the PHEV include battery, electric motor, and inverter losses. These losses can be divided into three types. The first type is the frictional and windage loss in the electric motor, which is a function of motor speed and load torque. The second type is the magnetic loss in the motor, which is related to the magnitude and frequency of the supply voltage. The last type is copper loss in the motor and internal loss in the battery due to battery internal resistance. This last type of loss is proportional to the current squared, i.e., out power squared if the voltage is assumed to be constant. Hence, the total electric system losses include a portion that

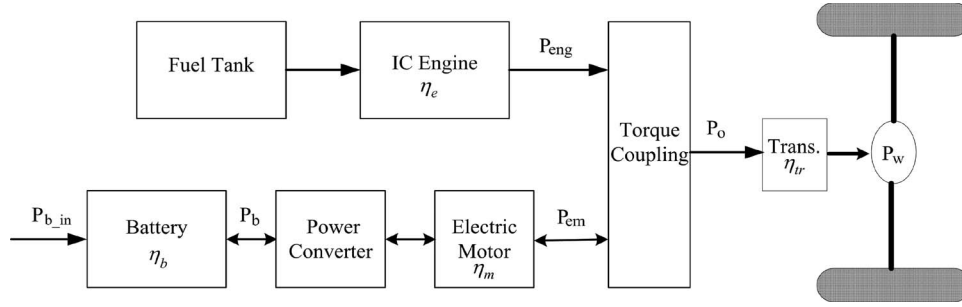


Fig. 1. Parallel HEV powertrain architecture, where P_{eng} is the engine power, P_b is the battery power, P_{b_in} is the total electrical power, P_{em} is the electric motor mechanical power, P_{eng} is the engine output power, P_o is the total output power to the transmission, η_e is the engine efficiency, η_b is the battery efficiency, η_m is the motor efficiency (including inverter), and η_{tr} is the transmission and drive line efficiency.

is constant (windage loss and some magnetic loss), a second portion that is proportional to the output power (a portion of frictional loss and some magnetic loss), and a third portion that is proportional to the square of the output power (copper and battery losses).

Therefore, the modeled losses, an approximation to true losses (always positive) in the most efficient electric drive operations for the given mechanical power outputs P_o , can be approximated as a second-order polynomial. For the analytic part of this paper, it is assumed that

$$P_b = P_{em} + Loss(P_{em}) = P_{em} + L_0 + AP_{em} + BP_{em}^2. \quad (1)$$

It should be emphasized that the nonlinear term in the loss function plays an important role in the optimization, as revealed in later sections. The linear term is usually less significant than the quadratic term resulting from losses such as copper and battery ohmic losses. The proposed approximation of the system electric power losses simply describes the fact about the existence of system peak efficiency, and it is the simplest nonlinear form that allows analytic solutions.

B. Vehicle Power Distribution Function

In a typical drive cycle with zero initial speed and zero final speed, the distribution of vehicle power demand is shown in Fig. 2. Certain characteristics of the distribution are common to all cycles with zero initial and final speeds. First, there must be a net energy consumed in the cycle, and therefore, the average power of the cycle must be positive. Second, occurrences of extreme positive power and extreme negative power occur less than the rest. In obtaining the optimal solutions, only a general distribution is assumed. In the simulation section, the distributions of vehicle output power for a given total energy consumption are modeled as a Cauchy distribution or a superposition of Cauchy distributions limited by the minimum and maximum powers, as shown in Fig. 3.

Specifically, the shadow area $\Phi(P_o)dP_o$ represents the time that the transmission output power is within the interval of P_o and $P_o + dP_o$. Therefore, the total vehicle operation time in one drive cycle is given as the integration of time over the whole power range

$$T = \int_{P_{min}}^{P_{max}} \Phi(P_o)dP_o. \quad (2)$$

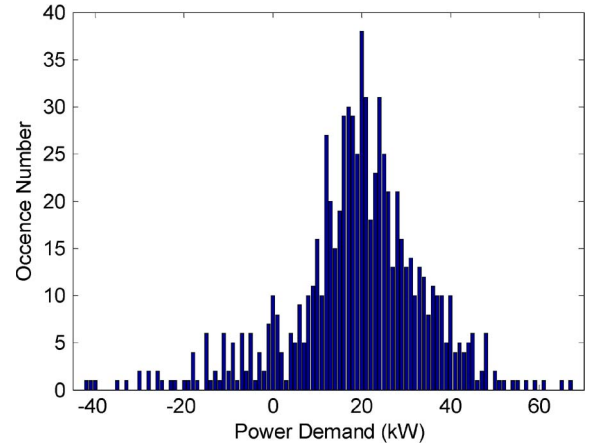


Fig. 2. Vehicle power distributions.

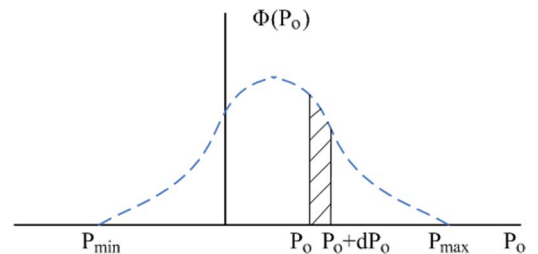


Fig. 3. Idealized vehicle power demand distributions.

In this driving cycle, the average output power \bar{P}_o is

$$\begin{aligned} \bar{P}_o &= \frac{\int_0^T P_o dt}{T} = \frac{\int_{P_{min}}^{P_{max}} P_o \Phi(P_o) dP_o}{T} \\ &= \frac{\int_{P_{min}}^{P_{max}} P_o \Phi(P_o) dP_o}{\int_{P_{min}}^{P_{max}} \Phi(P_o) dP_o}. \end{aligned} \quad (3)$$

C. ICE Fuel Consumption Characteristics

The fuel consumption rate of a nominal engine mainly depends on engine speed and torque. If the engine operates efficiently, the fuel consumption rate mainly depends on the engine output power P_{eng} . In this paper, it is assumed that the fuel consumption rate depends on P_{eng} only, as shown in Fig. 4.

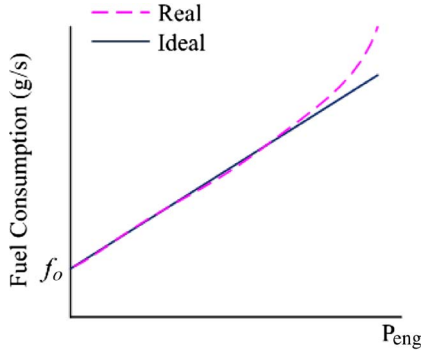


Fig. 4. Fuel consumption of a nominal engine.

Here, a linear relationship is applied to obtain the optimal solutions in a closed form

$$f = f_0 + kP_{\text{eng}} \quad (4)$$

where the intercept f_0 reflects the fuel consumption in engine idle, and the slope k is a constant that reflects the combustion efficiency approximately. A more accurate engine model, i.e., the piecewise linear model, will be discussed in Section IV, i.e.,

$$f = \begin{cases} f_0 + kP_{\text{eng}} & P_{\text{eng}} \leq P_1 \\ k_1P_{\text{eng}} & P_{\text{eng}} > P_1. \end{cases} \quad (5)$$

D. Power Strategy

In a simplistic view, the essence of HEV operating strategy is to determine when and how to run the engine in real time to fulfill the driver's request in terms of vehicle output torque (or power) while maintaining battery SOC within a range and minimizing frictional braking. Battery energy depletion targets are introduced into the operating strategy for the case of PHEV. In this paper, the control strategy is characterized by a pair of parameters P_s and P_c , with P_s being the threshold of transmission output power above which the engine is running to propel the vehicle while maintaining a constant motor mechanical power P_c . This simple strategy captures the essence of the more complicated and more realistic HEV control strategy and allows the optimization problem to be formulated and solved analytically. This strategy in one drive cycle is shown in Fig. 5.

P_{em} can be expressed as a linear piecewise function

$$P_{\text{em}} = \begin{cases} P_{\text{em min}}, & P_o \leq P_{\text{em min}} \\ P_o, & P_{\text{em min}} < P_o \leq P_s \\ P_c, & P_s < P_o \leq P_{\text{em max}} \end{cases} \quad (6)$$

$$P_{\text{eng}} = \begin{cases} 0, & P_o \leq P_s \\ P_o - P_c, & P_o > P_s \end{cases}$$

where $P_{\text{em min}}$ is the maximum regenerative power, P_s is the vehicle output power threshold above which the engine will be turned on, and P_c is the constant motor mechanical power during engine running. It is worth to point out that this P_c can be positive (discharging the battery) or negative (charging the battery).

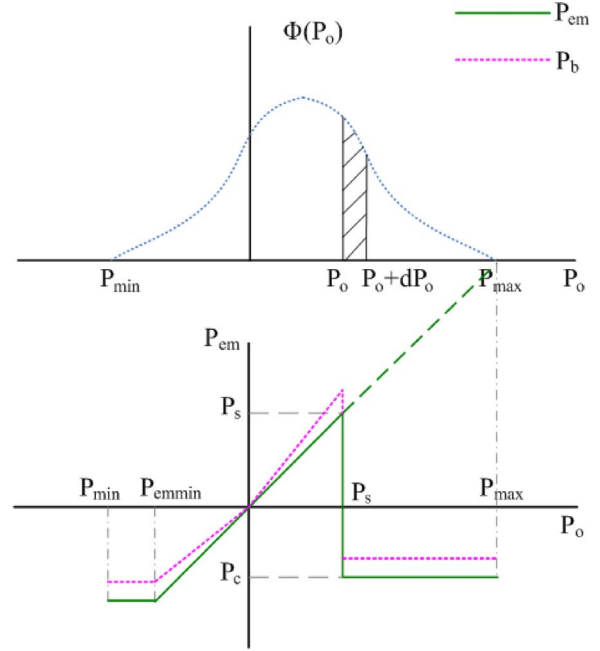


Fig. 5. Power management strategy used in this paper.

E. Total Fuel Consumption and Total Battery Energy

By definition, the engine is off if P_o is less than the threshold P_s ; therefore, the total fuel consumption in a drive cycle can be obtained as

$$\begin{aligned} X(P_s, P_c) &= \int_0^T f(t)dt = \int_{P_s}^{P_{\text{max}}} f(P_{\text{eng}})\Phi(P_o)dP_o \\ &= \int_{P_s}^{P_{\text{max}}} f(P_o - P_c)\Phi(P_o)dP_o. \end{aligned} \quad (7)$$

The total net battery energy consumed in this driving cycle can be obtained as the integral of battery power P_b over the whole drive cycle $[0, T]$ and is considered as a constant

$$E_b(P_s, P_c) = \int_0^T P_b dt = \int_{P_{\text{min}}}^{P_{\text{max}}} P_b \Phi(P_o)dP_o = \text{const.} \quad (8)$$

The preceding equation can be expanded as

$$\begin{aligned} E_b(P_s, P_c) &= \int_0^T P_b dt = \int_{P_{\text{min}}}^{P_{\text{max}}} P_b \Phi(P_o)dP_o \\ &= \int_{P_{\text{min}}}^{P_{\text{max}}} [P_{\text{em}} + \text{Loss}(P_{\text{em}})] \Phi(P_o)dP_o. \end{aligned} \quad (9a)$$

Equations (6) and (9a) yield

$$E_b(P_s, P_c) = \int_{P_{\text{min}}}^{P_{\text{em min}}} [P_{\text{em min}} + \text{Loss}(P_{\text{em min}})] \Phi(P_o)dP_o$$

$$\begin{aligned}
& + \int_{P_{em \min}}^{P_s} [P_o + \text{Loss}(P_o)] \Phi(P_o) dP_o \\
& + \int_{P_s}^{P_{\max}} [P_c + \text{Loss}(P_c)] \Phi(P_o) dP_o. \quad (9b)
\end{aligned}$$

In this paper, the loss function is approximated as a second-order polynomial

$$\text{Loss}(x) = L_o + Ax + Bx^2, \quad x = P_{em \min} \text{ or } P_o \text{ or } P_c. \quad (10)$$

The maximum net battery energy needed for all electric drive $E_{b \max}$ is introduced for convenience and is given as follows. $E_{b \max}$ is obtained by assuming that the vehicle is driven by battery/motor only throughout the drive cycle without turning on the engine, i.e.,

$$\begin{aligned}
E_{b \max}(P_s, P_c) &= E_b(P_{\max}, 0) \\
&= \int_{P_{\min}}^{P_{em \min}} [P_{em \min} + \text{Loss}(P_{em \min})] \Phi(P_o) dP_o \\
&+ \int_{P_{em \min}}^{P_{\max}} [P_o + \text{Loss}(P_o)] \Phi(P_o) dP_o. \quad (11)
\end{aligned}$$

Obviously, $E_{b \max}$ is a constant for a given drive cycle. The difference between E_b and $E_{b \max}$ is

$$\begin{aligned}
E(P_s, P_c) &= E_{b \max}(P_{\max}, 0) - E_b(P_s, P_c) \\
&= \int_{P_{em \min}}^{P_{\max}} [P_o + \text{Loss}(P_o)] \Phi(P_o) dP_o \\
&- \int_{P_{em \min}}^{P_s} [P_o + \text{Loss}(P_o)] \Phi(P_o) dP_o \\
&- \int_{P_s}^{P_{\max}} [P_c + \text{Loss}(P_c)] \Phi(P_o) dP_o \\
&= \int_{P_s}^{P_{\max}} [P_o + \text{Loss}(P_o)] \Phi(P_o) dP_o \\
&- \int_{P_s}^{P_{\max}} [P_c + \text{Loss}(P_c)] \Phi(P_o) dP_o. \quad (12)
\end{aligned}$$

For a given E_b , $E(P_s, P_c)$ is also a constant, which is a constraint to be used in later sections.

F. Optimization Strategy

In this paper, the objective is to minimize the fuel consumption for constant battery energy depletion. Therefore, we can formulate the optimization problem as

$$\text{Minimize } \{X(P_s, P_c)\} \quad (13)$$

Subject to :

$$\frac{dE(P_s, P_c)}{dP_s} = 0. \quad (14)$$

The optimal solutions P_s^* and P_c^* that minimize $X(P_s, P_c)$ satisfy (13) and (14), where P_s^* is the optimal power threshold to turn on the engine. If $P_s = P_s^*$ and $P_c = P_c^*$, then

$$\frac{dX(P_s, P_c)}{dP_s} = 0. \quad (15)$$

The derivative of the total fuel consumption with respect to P_s can be obtained from (7) as

$$\begin{aligned}
\frac{dX(P_s, P_c)}{dP_s} &= -f(P_s - P_c) \Phi(P_s) \\
&+ \int_{P_s}^{P_{\max}} \frac{df(P_e)}{dP_e} \cdot \left(-\frac{dP_c}{dP_s} \right) \Phi(P_o) dP_o \\
&= -f(P_s - P_c) \Phi(P_s) \\
&- k_{\text{eff}} \int_{P_s}^{P_{\max}} \left(\frac{dP_c}{dP_s} \right) \Phi(P_o) dP_o \quad (16)
\end{aligned}$$

where k_{eff} , as defined in (16), is the effective slope of engine fuel consumption rate $f(P_{\text{eng}})$. The introduction of k_{eff} greatly simplifies the integration in (16). It is justified because the derivative of $f(P_{\text{eng}})$ is usually not a strong function of P_e in the range of interest (not too far away from peak efficiency). For the linear engine model described by (4), $k_{\text{eff}} = k$. For the piecewise linear engine model described by (5), which is to be used for later analysis and simulation, k_{eff} is bounded by $k \leq k_{\text{eff}} \leq k_1$. Although k_{eff} is treated as a system parameter to be determined by (16), the treatment should not weaken the general results of this paper.

From (14)

$$\begin{aligned}
\frac{dE}{dP_s} &= -[P_s - P_c + L(P_s) - L(P_c)] \Phi(P_s) \\
&+ \int_{P_s}^{P_{\max}} [-1 - L'] \frac{dP_c}{dP_s} \Phi(P_o) dP_o = 0. \quad (17)
\end{aligned}$$

That is

$$\begin{aligned}
&-[P_s - P_c + L(P_s) - L(P_c)] \Phi(P_s) \\
&- (1 + L') \int_{P_s}^{P_{\max}} \left(\frac{dP_c}{dP_s} \right) \Phi(P_o) dP_o = 0 \quad (18)
\end{aligned}$$

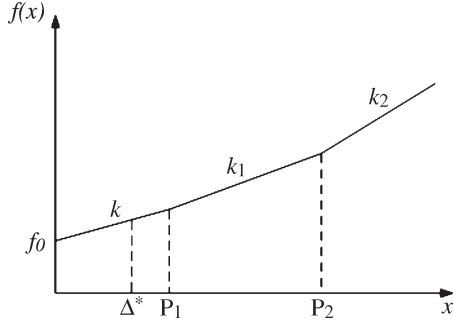


Fig. 6. Piecewise linear model of the engine fuel consumption rate.

where $L' = dL(x)/dx|_{x=P_c}$. Equations (16) and (18) yield

$$\frac{dX}{dP_s} = -f(P_s - P_c)\Phi(P_s) + \frac{k_{\text{eff}}}{1 + L'} [P_s - P_c + L(P_s) - L(P_c)] \Phi(P_s). \quad (19)$$

Assume $L(x) = L_0 + Ax + Bx^2$, so $L' = A + 2Bx$, i.e.,

$$\frac{dX}{dP_s} = -f(P_s - P_c)\Phi(P_s) + k_{\text{eff}}(P_s - P_c)\Phi(P_s) + \frac{k_{\text{eff}}B(P_s - P_c)^2}{1 + A + 2BP_c} \Phi(P_s). \quad (20)$$

Let $\Delta (= P_s - P_c)$ be the minimum engine power, i.e.,

$$\frac{dX}{dP_s} = \left[-f(\Delta) + k_{\text{eff}}\Delta + \frac{k_{\text{eff}}B}{1 + A + 2BP_c} \Delta^2 \right] \Phi(P_s). \quad (21)$$

Let optimal solutions be P_s^* and P_c^* and the optimal Δ be

$$\Delta^* = P_s^* - P_c^* \quad (22)$$

where Δ^* is the optimal minimum engine power below which the engine is off. Therefore, a general optimization solution can be obtained from

$$-f(\Delta^*) + k_{\text{eff}}\Delta^* + \frac{k_{\text{eff}}B}{1 + A + 2BP_c} \Delta^{*2} = 0. \quad (23)$$

A piecewise linear fuel consumption model, as depicted in the following figure, is used for further analysis and simulations. As shown in Fig. 6, f_0 is the engine idle fuel consumption rate, and k , k_1 , and k_2 are the local slopes of engine fuel consumption rate as a function of engine power. Within P_1 and P_2 , the engine has constant peak efficiency.

P_1 is one of the important engine characteristics and is the lowest engine output power with peak engine efficiency. P_1 is typically between 15 and 35 kW and depends on the engine size, with higher P_1 for bigger engines. The optimal solution has an intrinsic relationship to P_1 , which will be elaborated more in later sections. From the preceding figure, $f_0 + kP_1 = k_1P_1$; therefore

$$P_1 = \frac{f_0}{k_1 - k}. \quad (24)$$

Two special cases of the engine model are considered as follows.

- 1) Case for an ideal engine of constant efficiency. From (5), $f(x) = k_1x$. It is evident that $f' = k_1$ and $k_{\text{eff}} = k_1$. Therefore, $(dX/dP_s) = (k_1B\Delta^2/1 + A + 2BP_c)\Phi(P_s)$. In this case, the optimal solution is given by $\Delta^* = 0$.
- 2) Case for a piecewise linear engine model. Assuming that $P_2 > P_{\text{max}} - P_c$, then k_{eff} satisfies $k < k_{\text{eff}} < k_1$.

It can be shown that the optimal solutions satisfy that $\Delta^* \leq P_1$. For if $\Delta > P_1$, then the Δ that corresponds to the minimum fuel consumption is found as $\Delta = P_1$ based on (21) and case 1 analysis. Therefore, only the case of $\Delta \leq P_1$ should be considered for the optimization. It follows that

$$\frac{dX}{dP_s} = \left[-f_0 + (k_{\text{eff}} - k)\Delta + \frac{k_{\text{eff}}B}{1 + A + 2BP_c} \Delta^2 \right] \Phi(P_s). \quad (25)$$

Optimal solutions P_s^* and P_c^* satisfy

$$-f_0 + (k_{\text{eff}} - k)\Delta^* + \frac{k_{\text{eff}}B}{1 + A + 2BP_c} (\Delta^*)^2 = 0. \quad (26)$$

Rearranging (26), we can obtain the following equation:

$$-\frac{f_0}{k_1 - k} + \frac{(k_{\text{eff}} - k)}{k_1 - k} \Delta^* = -\frac{k_{\text{eff}}}{k_1 - k} \cdot \frac{B\Delta^{*2}}{1 + A + 2BP_c}. \quad (27)$$

The following inequality is true, as derived from (16) and (19), i.e., $-P_1 + ((k_{\text{eff}} - k)/k_1 - k)\Delta^* < 0$. Since $((k_{\text{eff}} - k)/k_1 - k) \approx 1$, we have

$$\Delta^* < P_1. \quad (28)$$

Therefore, if $B > 0$, then the optimal $(P_s^* - P_c^*)$ should be less than P_1 . This will be verified in the simulation sections.

If B is small, a good approximation of the optimal solution can be obtained as follows:

$$-P_1 + \Delta^* = -\frac{k_1}{f_0} P_1 \frac{B\Delta^{*2}}{1 + A} \quad \Delta^* \approx P_1 \left(1 - \frac{k_1}{f_0} \frac{BP_1^2}{1 + A} \right). \quad (29)$$

Recall that Δ is the minimum engine output power for engine-on operations, the optimal value of Δ is determined by (26), and it is related to system parameters approximately by (29). It clearly shows that the optimal Δ^* is lower than P_1 and approaches P_1 as the electric system becomes more efficient. To reduce the electric loss, P_s should be reduced, and P_c should be increased to maintain the same net battery energy depletion; therefore, Δ is reduced to a lower level. The optimal Δ is reached if further reduction in Δ results in too much loss in engine efficiency due to $P_e < P_1$. A better approximation about the optimal Δ can be obtained from (27), i.e.,

$$\Delta^* = \frac{-1 + \sqrt{1 + 4P_1^2 k_1 B' / f_0}}{2(k_1 P_1 B' / f_0)} \quad (30)$$

where $B' = B/(1 + A)$.

Equation (30) or (29) as an approximation establishes one of the conditions that optimal P_s and P_c must satisfy. It is established that $(P_s^* - P_c^*)$ determines the optimality and is only determined by powertrain characteristics. Drive cycle properties and battery energy depletion target affect P_s^* and P_c^* but not $(P_s^* - P_c^*)$.

Together with (30) and (12), the optimal solutions P_s^* and P_c^* can be completely determined. The main results so far obtained, as captured in the following, bear significance to general PHEV applications.

- 1) $P_s^* - P_c^*$ is the optimal minimum power that the engine outputs in engine-on operations. Since it does not depend on drive cycle properties and the battery energy depletion target, in principle, it can be calibrated using basic system characteristics, and it should be valid for all drive cycles and all CD targets.
- 2) P_1 as the lowest engine output power with peak efficiency is of particular importance, and the optimal minimum engine power $P_s^* - P_c^*$ is always less than this characteristic power P_1 . This property provides a good reference for calibrating $P_s^* - P_c^*$.
- 3) P_s or P_c can be calibrated to achieve intended battery depletion targets for intended drive cycles, or can be found through adaptive controls, whereas $P_s - P_c$ is maintained at the optimal level $P_s^* - P_c^*$. Conceptually, P_c can be scheduled, P_s can be determined from $(\Delta^* + P_c)$, and the observed charge-depleting rate is used to adjust P_c to achieve the desired charge-depleting target without compromise in efficiency. Of course, that requires that the trip lasts longer than relevant time scales.

In real-world driving, the trip distance and energy consumption are not precisely known. Modern vehicular navigation system may provide trip information to be used by the CD strategies. Since the proposed strategy requires only the trip distance and the AER (or battery energy content), it is feasible to implement this control strategy for real vehicle applications using the estimated trip information.

III. MODEL SETUP FOR THE POWERTRAIN COMPONENTS

In the following, all the system parameters used to construct the simulation model are obtained from real-world experiments. The model characteristics and parameters are described as follows. For a given set of system characteristics, power distribution characteristics, and net battery energy depletion, a pair of optimal P_s^* and P_c^* that yields minimal fuel consumption can be solved.

A. Electric Drive System Loss Model Characteristics

The total system power loss of an electric driver system includes motor, inverter, and battery losses. Fig. 7 shows the losses of a nominal electric drive system and an improved electric drive system, which are modeled as a second polynomials of the system mechanical power to describe the minimum system loss for a given mechanical power output, as if the

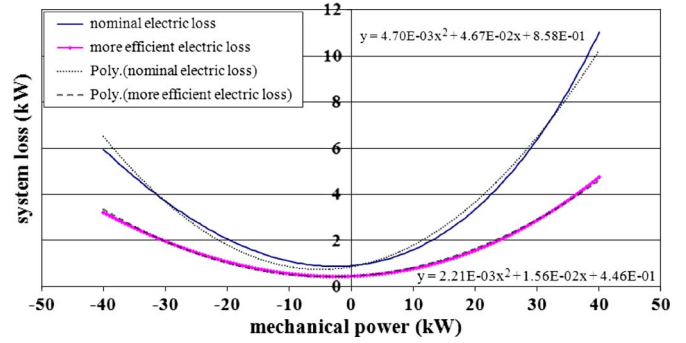


Fig. 7. Electric drive system loss models.

TABLE I
ELECTRIC SYSTEM LOSS MODEL

	Baseline (ES1)	Improved (ES2)	Improved (ES3)
V_0 (V)	345	345	345
R (ohms)	0.3	0.3	0.15
L_0 (kW)	0.86	0.42	0.45
A	0.0467	0.0297	0.0156
B (1/kW)	0.0047	0.00366	0.00221

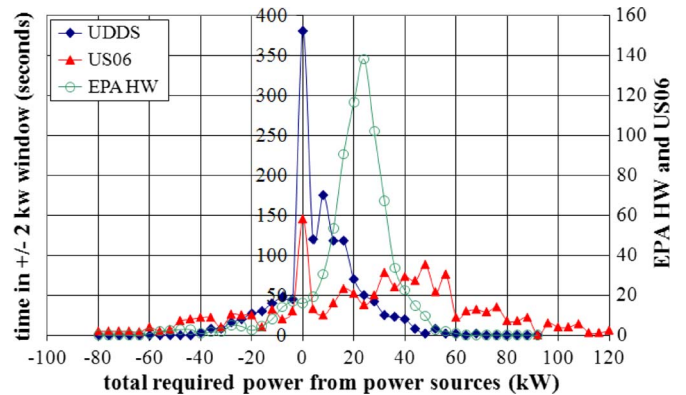


Fig. 8. Output power distribution in UDDS, EPA HW, and US06.

electric machine is coupled with an ideal continuous variable transmission (CVT) with 100% efficiency and able to operate at the optimal speed and torque for that mechanical power. The loss system parameters are shown in Table I, where V_0 is the battery nominal voltage, and R is the nominal dc impedance.

B. Output Power Distribution Model

The distribution of the required output power for a given drive cycle, as defined in Section II, is used to characterize the drive cycle. Cycle properties such as total energy consumption, total drive cycle time, and average power can be obtained from this distribution function. The distributions of P_o from the nominal vehicle in three common driving-cycle tests such as United States Dynamometer Driving Schedule (UDDS), the U.S. Environmental Protection Agency (EPA) Highway (HW), and US06, are shown in Fig. 8.

For a given total energy, the distribution of P_o can be modeled as a Cauchy distribution or superposition of Cauchy distribution, limited by the minimum and maximum powers.

TABLE II
 DRIVE CYCLE DETAILS

	h (1/kj)	P_{ave} (kW)	P_w (kW)	P_{min} (kW)	P_{max} (kW)	T (sec)	E (MJ)
UDDS1	108.3	7.1	9	-40	70	2741	21.92
UDDS2	74.3	6.45	14	-40	70	2740	21.93
HW1	30.3	20.5	9	-60	60	765.7	14.00
HW2	20.85	22.2	14	-60	60	765.0	14.02

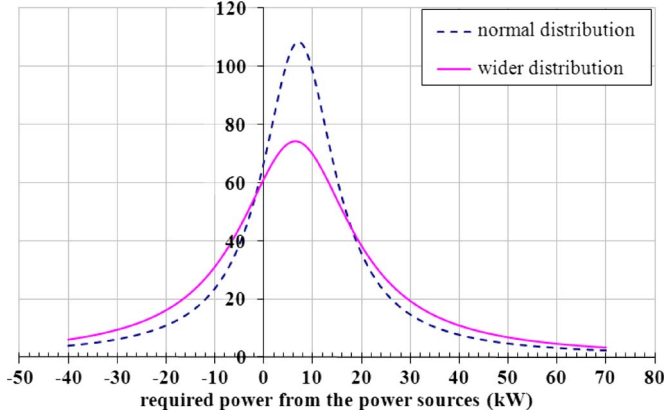


Fig. 9. Normal and wider distribution in UDDS.

The distribution function is characterized by the peak power, average power, and the power width at half height, i.e.,

$$\Phi(P_o) = \frac{h}{1 + \left(\frac{P_o - P_{ave}}{P_w}\right)^2} \quad \text{for } P_{min} \leq P_o \leq P_{max} \quad (31)$$

where h is the peak value of $\Phi(P_o)$, P_{ave} is the average power, and P_w is the half width of the peak (at a half height).

The vehicle operation time and the total energy Ω in this drive cycle are given by

$$T = \int_{P_{min}}^{P_{max}} \Phi(P_o) dP_o = hP_w \arctan\left(\frac{P_o - P_{ave}}{P_w}\right) \Big|_{P_o=P_{min}}^{P_o=P_{max}} \quad (32)$$

$$e = \int_{P_{min}}^{P_{max}} P_o \Phi(P_o) dP_o = \left\{ \frac{hP_w^2}{2} \ln \left[1 + \left(\frac{P_o - P_{ave}}{P_w}\right)^2 \right] + hP_w P_{ave} \arctan\left(\frac{P_o - P_{ave}}{P_w}\right) \right\} \Big|_{P_o=P_{min}}^{P_o=P_{max}} \quad (33)$$

The parameters in Table II are used to model normal and wider power distributions with the same total energy and time operation in UDDS and EPA HW drive cycles. Here, “1” means the normal power distributions, and “2” means the wider power distributions. More aggressive driving tends to yield wider power distributions with more occurrence of quick accelerations and decelerations. The distributions for UDDS and EPA HW are shown in Figs. 9 and 10, respectively.

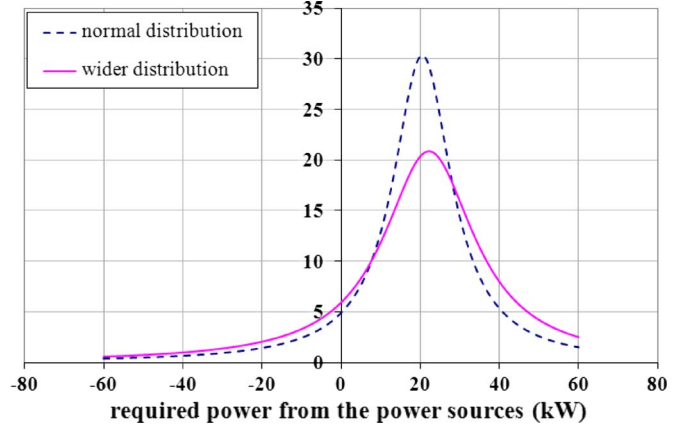


Fig. 10. Normal and wider distribution in EPA HW.

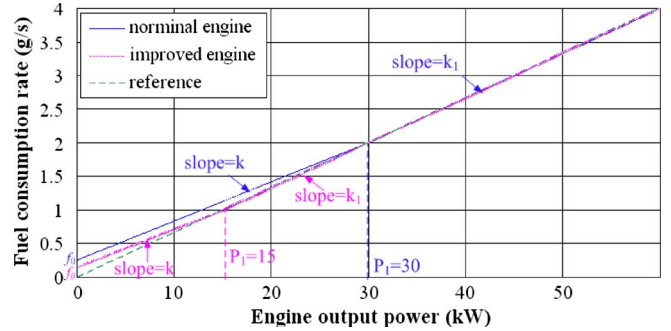


Fig. 11. Fuel consumption rate at different engine output powers.

 TABLE III
 ENGINE FUEL RATE PARAMETERS

	Nominal Engine	Improved Engine
f_0 (grams/s)	0.26	0.15
K (grams/s/kW)	0.058	0.05667
P_1 (kW)	30	15
K_1 (g/s/kW)	0.06667	0.06667

C. Engine Model Characteristics

A piecewise linear relationship between fuel consumption rate and engine output power is considered. Two different engines having the same peak efficiency, i.e., nominal engine and improved engine, are modeled in Fig. 11, and the modeling parameters are listed in Table III. Similar to the idealized electric machine described in this section, the engine operates as if it is coupled with an ideal CVT. This simple model intends to capture essential characteristics such as idle fuel consumption rate, peak efficiency, and the minimum power to reach the peak efficiency.

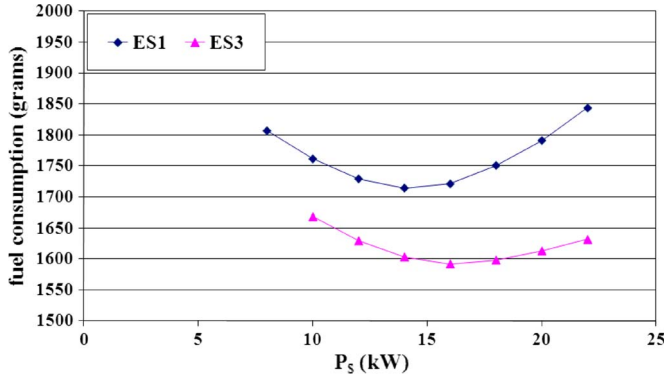


Fig. 12. Fuel consumption versus engine output power in UDDS1 with zero battery net energy.

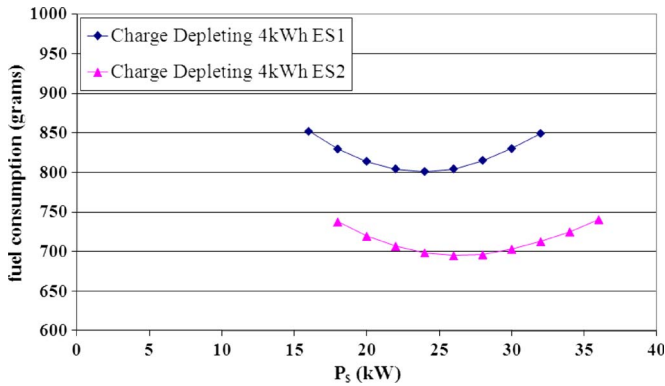


Fig. 13. Fuel consumption versus engine output power in UDDS1 with 4-kWh battery net energy.

The parameters f_o , k , P_1 , and k_1 are marked in Fig. 11 and will be used for engine piecewise linear model discussion in the next section.

IV. RESULTS AND DISCUSSION

Minimizing the total fuel consumption in a drive cycle while maintaining a constant battery net energy leads to optimal solutions for a given set of system parameters and output power distribution. This section will discuss the characteristics of the optimal solutions.

A. General Properties of Optimal Solutions (P_s^* , P_c^*) in UDDS Driving Cycle

We first look at the charge-sustaining operation of a PHEV. In other words, the net battery energy consumed in the whole drive cycle is zero. Fig. 12 shows the dependence of the total fuel consumption on P_s in cases of UDDS1 drive cycle, with nominal engine and with different electric losses (baseline electric drive ES1 and improved electric drive ES3).

In the following, we look at the fuel consumption during charge-depleting mode. Fig. 13 shows the dependence of the total fuel consumption on P_s for the previously indicated cases (ES1 and ES3) during UDDS1 drive cycle in charger depletion

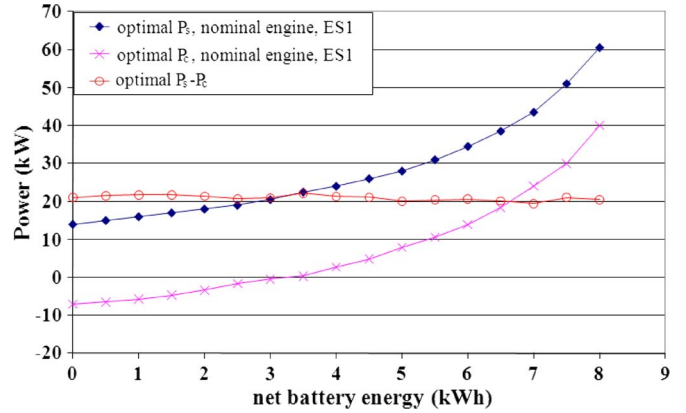


Fig. 14. Optimal P_s^* , P_c^* , and $P_s^* - P_c^*$ at different net available battery energies.

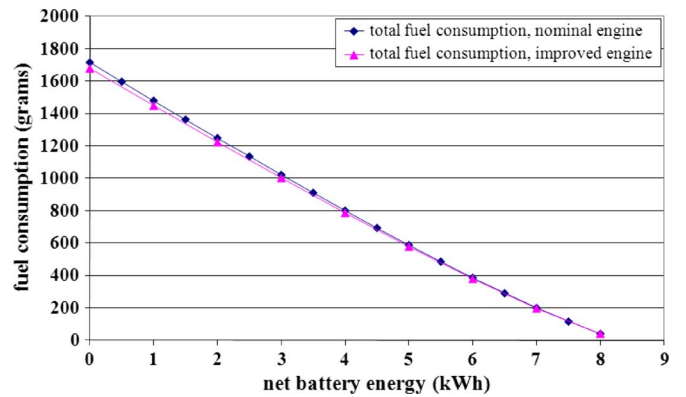


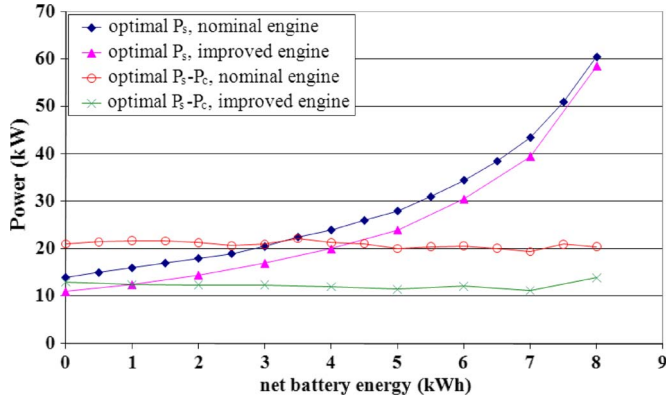
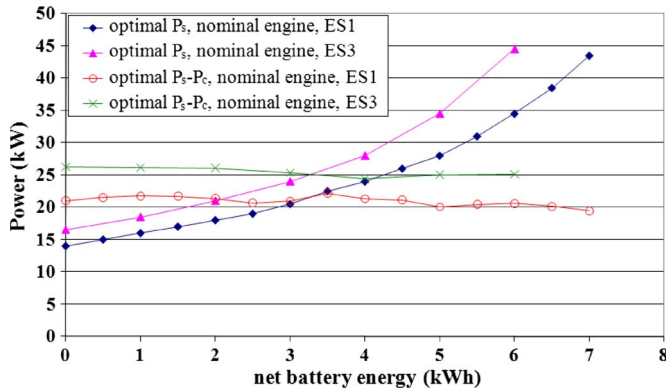
Fig. 15. Fuel consumption versus net battery energy for different engines.

mode with a total of 4-kWh battery energy consumed during the whole drive cycle.

As a result, the total fuel consumption is reduced by using optimal P_s^* and P_c^* . It reduces by around 5% in case of zero net battery energy and 7% in case of charge-depleting 4-kWh net battery energy. The higher electric loss model results in higher fuel consumption. In addition, the higher electric loss model tends to have a higher sensitivity or curvature at the optimal P_s^* . This can be explained by the dependence of the local curvature on electric loss coefficients A and B .

With the UDDS1 drive cycle, nominal engine, and baseline electric drive losses, the optimal P_s^* and P_c^* at different net battery energies are shown in Fig. 14. Both optimal P_s^* and P_c^* increase with the increase of net battery energy, yet $P_s^* - P_c^*$ has almost no dependence on the net available battery energy, as expected. $P_s^* - P_c^*$ mainly depends on engine characteristics and electric loss coefficient B .

With the same drive cycle UDDS1 and electric driving loss (ES1) parameters, the fuel consumptions for the nominal engine and the improved engine are shown in Fig. 15. As a result, the improved engine only improves the fuel consumption slightly, i.e., by about 2% at the low net battery energy. At the higher net battery energy, the improvement is minor since the engine operates at high output power in this situation, and therefore, the fuel consumption for improved engine is very close to that for the nominal engine.


 Fig. 16. Optimal P_s^* and $P_s^* - P_c^*$ versus net battery energy for different engines.

 Fig. 17. Optimal P_s^* and $P_s^* - P_c^*$ versus net battery energy for the different electric losses.

B. Impacts of Vehicle Properties on Optimal Solutions in UDDS Driving Cycle

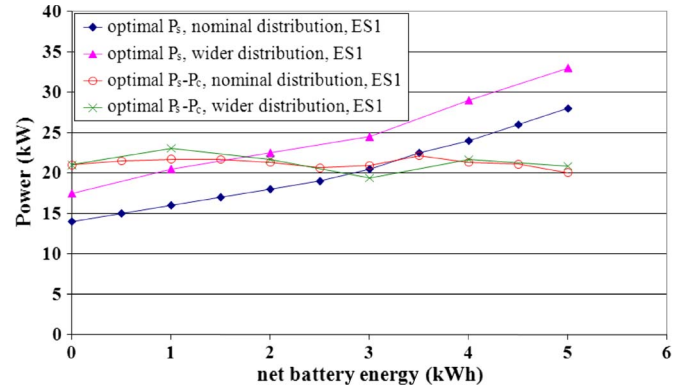
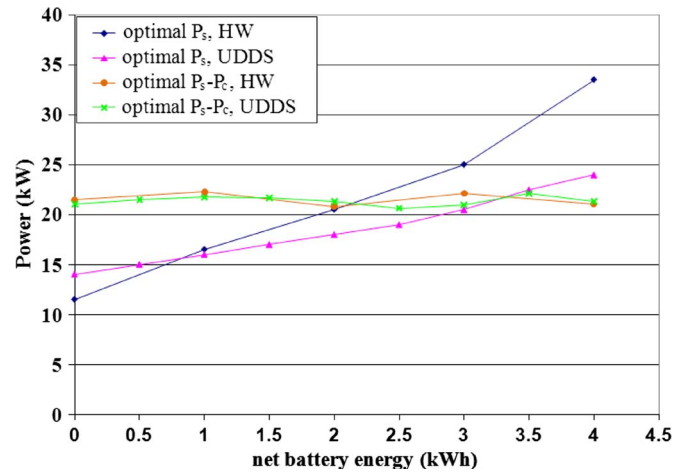
The impacts of vehicle system properties on P_s^* and $P_s^* - P_c^*$ will be discussed next. Here, the vehicle system properties include electric driving system losses, power distributions, and engine models. Results will be in turn shown for the following cases. Fig. 16 shows the effect of engine characteristics on optimal solutions. As expected from (29), for a system with an engine of lower P_1 , ($P_s^* - P_c^*$) is lower.

As shown in Fig. 17, optimal solutions P_s^* with low electric loss (ES3) are higher than baseline (ES1) solutions because the lower electric loss results in higher electric output power. In addition, solutions $P_s^* - P_c^*$ with ES3 are higher than ES1 solutions since $P_s^* - P_c^*$ depends inversely on the electric loss coefficient B , as shown in (29) and (30).

The effect of the different power distribution models on the optimal solutions is shown in Fig. 18. It can be seen from this figure, in the case of wider power distribution UDDS2, that the optimal P_s^* is higher than the values for normal distribution, but the optimal $P_s^* - P_c^*$ remains the same. That is because the optimal $P_s^* - P_c^*$ is only influenced by engine properties and system electric loss models.

C. Sensitivity of Driving Cycles on Optimal Solutions

All the results previously shown are derived in the UDDS driving cycle. For a given net battery energy, the sensitivity of


 Fig. 18. Optimal P_s^* and $P_s^* - P_c^*$ versus net battery energy for the different power distributions.

 Fig. 19. Optimal P_s^* and $P_s^* - P_c^*$ versus net battery energy for UDDS and HW driving cycles.

different driving cycles (UDDS and highway) on the optimal solutions is also investigated and shown in Fig. 19.

Fig. 19 provides the optimal solutions for the city (UDDS) and highway (HW) driving cycles. It is clear that these cycles represent different driving conditions, such as the large variation in maximum and minimum power, average speed, and cycle distance. As a result, significant difference on optimal solutions P_s^* would be expected. Optimal solutions are highly dependent on the drive cycles, but there is no big difference for optimal $P_s^* - P_c^*$. That is because the optimal $P_s^* - P_c^*$ is only influenced by engine properties and system electric loss models but not by the details of the driving cycle.

D. Verification of $P_s^* - P_c^*$ Approximation

For any power distribution and system property characterized by this study, the optimal $P_s^* - P_c^*$ that minimizes the total fuel for constant battery energy is given by (30).

The following approximation with reasonable accuracy can be utilized to obtain the optimal ($P_s^* - P_c^*$) in the piecewise linear engine model:

$$P_s^* - P_c^* \approx \frac{k - k_{\text{eff}} + \sqrt{(k - k_{\text{eff}})^2 + 4k_{\text{eff}}B'f_0}}{2k_{\text{eff}}B'} \quad (34)$$

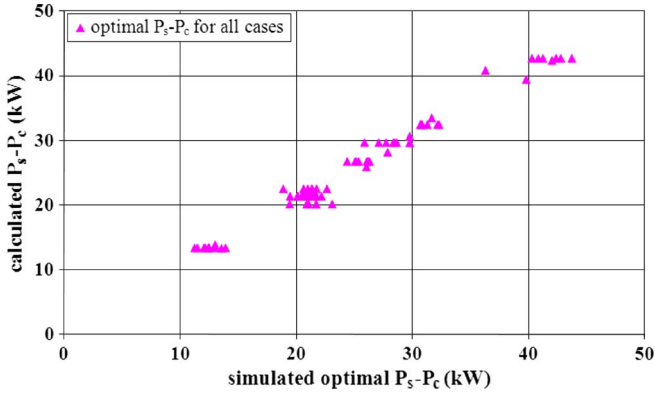


Fig. 20. Comparison between simulated $P_s^* - P_c^*$ and calculated $P_s^* - P_c^*$ using the approximation.

where $B' = B/(1 + A)$, and $k < k_{\text{eff}} < k_1$. The parameter k_{eff} is estimated from (16). Fig. 20 shows the comparison between simulated $P_s^* - P_c^*$ and calculated $P_s^* - P_c^*$ for all simulation cases, where the horizontal axis is the simulated $P_s^* - P_c^*$ with the optimal solution, and the vertical axis is the calculated $P_s^* - P_c^*$ approximated from (34).

E. Case for Constant Engine Power

The method developed in this paper can be used to investigate other control strategies. In the case of constant engine power, the fuel consumption and battery energy can be expressed in terms of P_s and P_{eng} , and $P_c = P_o - P_{\text{eng}}$.

This strategy is less efficient because of the higher electric losses due to the nonconstant P_c . Therefore, this strategy is not explored further.

F. Effectiveness and Validity of the Analytical Solution

To confirm the effectiveness and validity of the proposed analytical solutions, simulations are carried out for a midsize Sport Utility Vehicle using PSAT simulation software. Three different driving cycles are simulated, including UDDS, US06 and CR City Cycle. For the purpose of comparing fuel consumption results with the proposed strategy, the fuel consumption obtained with the default controller in ADVISOR (which is an electric dominate based strategy [39]) is taken as the baseline. The net battery energy available is 6 kWh, and the distance is 37.25 mi for five UDDS cycles, 40.05 mi for five US06 cycles, and 40 mi for CR City cycle.

For fair comparison, the battery final SOC must be at the same level, and therefore, SOC correction is necessary. The linear regression method was used to ensure that the initial and final SOC are the same [39]. In this paper, the initial SOC is 100%, and the target SOC is 30%, and therefore, the difference between the final and target SOC is considered. Linear fitting was adopted to obtain fuel consumption and corrected with SOC.

The power demand, motor torque, and engine torque for the UDDS driving cycle is shown in Fig. 21. The simulated fuel consumption results are shown in Table IV. It can be seen that the proposed strategy improves on average by 8.7%. The fuel savings shown in Table IV obtained by the proposed strategy

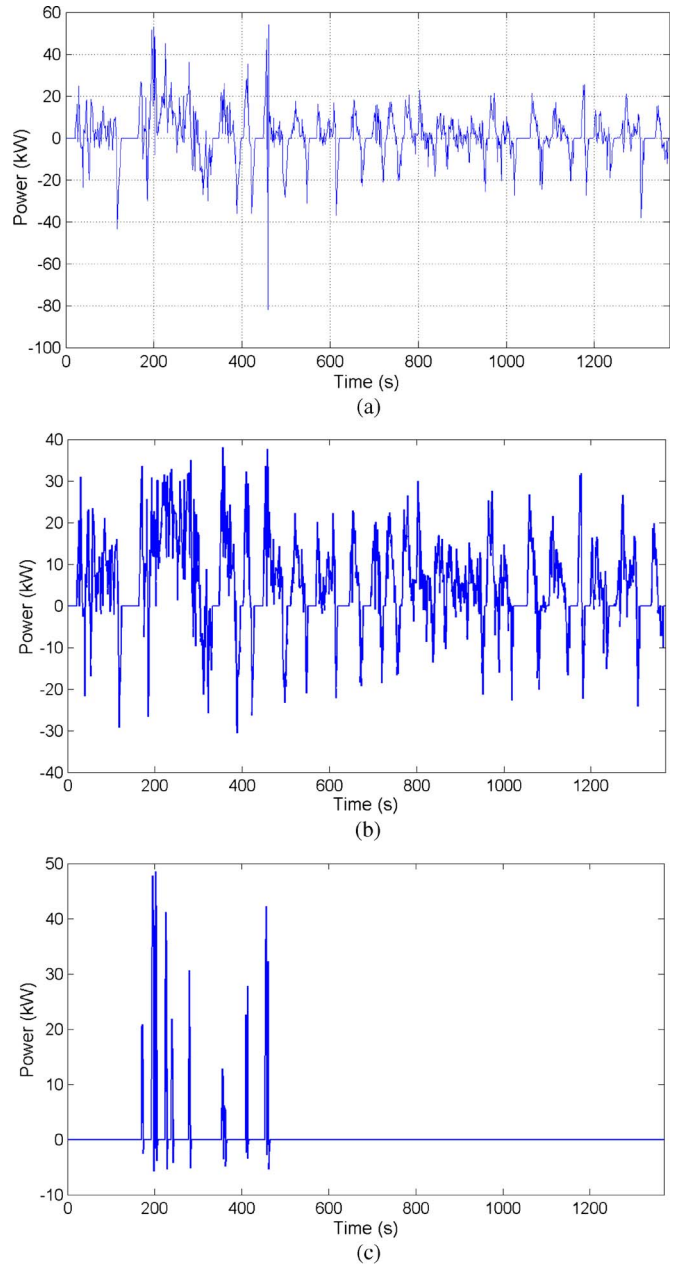


Fig. 21. Simulated vehicle power demand, motor power, and engine power for the UDDS cycle. (a) Total power demand. (b) Motor power. (c) Engine power.

TABLE IV
TYPICAL DRIVE CYCLE SIMULATION RESULTS

Drive cycle	Fuel consumption (kg) (Base strategy)	Fuel consumption (kg) (Proposed control)	Fuel savings (%)
5 UDDS cycles	2.25	2.02	10.2
CR City	5.72	5.25	8.2
5US06 Cycles	5.47	5.05	7.7

is primarily due to the reduction in electric system losses. As discussed earlier, the electric system loss increases significantly as the power increases.

The error between fuel consumption results from the analytical solutions directly (see Fig. 15) and the one obtained from simulation in PSAT by incorporating the proposed control strategy (Table IV) is generally less than 3.0%. This therefore confirms the validity of the proposed method and the simplified models used to derive the solutions.

V. CONCLUSION

This paper has analyzed the minimization of fuel consumption for a parallel ICE–electric powertrain. We have theoretically derived the optimal power solutions (P_s^* and P_c^*) for the given characteristics of electric losses, engine fuel consumption rate, and drive cycles. It is found that $P_s^* - P_c^*$ is the controlling factor in minimizing the total fuel consumption for the given battery energy depletion targets, and that $P_s^* - P_c^*$ is determined solely by powertrain characteristics. The simulation results show that the fuel economy can be improved definitely for HEVs and PHEVs with the optimal power solutions, as this strategy guarantees the optimal solutions for any constant battery energy depletion and any drive cycles. $P_s^* - P_c^*$ is the optimal minimum power that the engine outputs in engine-on operations.

Since it does not depend on drive cycle properties and the battery energy depletion target, in principle, it can be calibrated for all applications. P_1 , as the lowest engine output power with peak efficiency, is of particular importance, and the optimal minimum engine power $P_s^* - P_c^*$ is less than the characteristic power P_1 and approaches P_1 for efficient electric drive systems. This relationship provides a basis for calibrating $P_s^* - P_c^*$. Since $P_s^* - P_c^*$ is largely known and is constant, the optimal power management strategy problem is replaced with a much simpler problem, i.e., only P_s or P_c needs to be determined to achieve the intended battery depletion targets for the intended drive cycles by means of calibration or adaptive controls, while $P_s^* - P_c^*$ guarantees the most fuel efficient operations regardless of charge sustaining or charge depleting.

REFERENCES

- [1] V. Freyermuth, E. Fallas, and A. Rousseau, "Comparison of powertrain configuration for plug-in HEVs from a fuel economy perspective," presented at the SAE World Congr. Exh., Detroit, MI, 2008, Paper SAE 2008-01-0461.
- [2] F. U. Syed, M. L. Kuang, and J. Czubay, "Derivation and experimental validation of a power-split hybrid electric vehicle model," *IEEE Trans. Veh. Technol.*, vol. 55, no. 6, pp. 1731–1747, Nov. 2006.
- [3] J. Meisel, "An analytic foundation for the two-mode hybrid-electric powertrain with a comparison to the single-mode Toyota Prius THS-II," presented at the SAE World Congr. Exh., Detroit, MI, 2009, Paper SAE 2009-01-1321.
- [4] T. Katrašnik, "Hybridization of powertrain and downsizing of IC engine—A way to reduce fuel consumption and pollutant emissions—Part 1," *Energy Convers. Manage.*, vol. 48, no. 5, pp. 1411–1423, May 2007.
- [5] T. Katrašnik, F. Trenc, and S. R. Opresnik, "Analysis of energy conversion efficiency in parallel and series hybrid powertrains," *IEEE Trans. Veh. Technol.*, vol. 56, no. 6, pp. 3649–3659, Nov. 2007.
- [6] C.-C. Lin, H. Peng, J. W. Grizzle, and J.-M. Kang, "Power management strategy for a parallel hybrid electric truck," *IEEE Trans. Control Syst. Technol.*, vol. 11, no. 6, pp. 839–849, Nov. 2003.
- [7] H. Zhao and B. Zhang, "Research on parameters matching of parallel hybrid electric vehicle powertrain," in *Proc. IEEE VPPC*, Sep. 3–5, 2008, pp. 1–4.
- [8] B. K. Powell, K. E. Bailey, and S. R. Cikanek, "Dynamic modeling and control of hybrid electric vehicle powertrain systems," *IEEE Control Syst. Mag.*, vol. 18, no. 5, pp. 17–33, Oct. 1998.
- [9] M. Ehsani and K. L. Butler, "Application of electrically peaking hybrid (ELPH) propulsion system to a full-size passenger car with simulated design verification," *IEEE Trans. Veh. Technol.*, vol. 48, no. 6, pp. 1779–1787, Nov. 1999.
- [10] Z. Song, W. Guangqiang, and Z. Songlin, "Study on the energy management strategy of DCT-based series-parallel PHEV," in *Proc. Int. Conf. CCIE*, Jun. 5–6, 2010, vol. 1, pp. 25–29.
- [11] C. Yang, J. Li, W. Sun, B. Zhang, Y. Gao, and X. Yin, "Study on global optimization of plug-in hybrid electric vehicle energy management strategies," in *Proc. APPEEC*, Mar. 28–31, 2010, pp. 1–5.
- [12] T. H. Bradley and A. A. Frank, "Design, demonstrations and sustainability impact assessments for plug-in hybrid electric vehicles," *Sustain. Renew. Energy Rev.*, vol. 13, no. 1, pp. 115–128, Jan. 2009.
- [13] A. Simpson, "Cost-benefit analysis of plug-in hybrid electric vehicle technology," presented at the 22nd Int. Battery, Hybrid Fuel Cell Electric Vehicle Symp. Exh., Yokohama, Japan, Oct. 23–28, 2006, Paper NREL/CP-540-40485.
- [14] S. S. Williamson, "Electric drive train efficiency analysis based on varied energy storage system usage for plug-in hybrid electric vehicle application," in *Proc. IEEE Power Electron. Spec. Conf.*, Jun. 17–21, 2007, pp. 1515–1520.
- [15] J. Gonder and T. Markel, "Energy management strategies for plug-in hybrid electric vehicles," presented at the SAE World Congr. Exh., Detroit, MI, 2007, Paper SAE 2007-01-0290.
- [16] J. Wu, N.-X. Cui, C.-H. Zhang, and W.-H. Pei, "PSO algorithm-based optimization of plug-in hybrid electric vehicle energy management strategy," in *Proc. 8th WCICA*, Jul. 7–9, 2010, pp. 3997–4002.
- [17] S. J. Moura, H. K. Fathy, D. S. Callaway, and J. L. Stein, "A stochastic optimal control approach for power management in plug-in hybrid electric vehicles," *IEEE Trans. Control Syst. Technol.*, vol. 19, no. 3, pp. 545–555, May 2011.
- [18] H. Banvait, S. Anwar, and Y. Chen, "A rule-based energy management strategy for Plug-in Hybrid Electric Vehicle (PHEV)," in *Proc. ACC*, Jun. 10–12, 2009, pp. 3938–3943.
- [19] S. A. Rahman, N. Zhang, and J. Zhu, "A comparison on fuel economy and emissions for conventional hybrid electric vehicles and the UTS plug-in hybrid electric vehicle," in *Proc. 2nd ICCAE*, Feb. 26–28, 2010, vol. 5, pp. 20–25.
- [20] R. Ghorbani, E. Bibeau, and S. Filizadeh, "On conversion of hybrid electric vehicles to plug-in," *IEEE Trans. Veh. Technol.*, vol. 59, no. 4, pp. 2016–2020, May 2010.
- [21] L. Zhang, C. Lin, and X. Niu, "Optimization of control strategy for plug-in hybrid electric vehicle based on differential evolution algorithm," in *Proc. APPEEC*, Mar. 27–31, 2009, pp. 1–5.
- [22] S. Stockar, V. Marano, G. Rizzoni, and L. Guzzella, "Optimal control for plug-in hybrid electric vehicle applications," in *Proc. ACC*, Jun. 30, 2010–Jul. 2, 2010, pp. 5024–5030.
- [23] F. Mapelli, M. Mauri, and D. Tarsitano, "Energy control strategies comparison for a city car plug-in HEV," in *Proc. 35th IEEE IECON*, Nov. 3–5, 2009, pp. 3729–3734.
- [24] P. B. Sharer and A. Rousseau, "Plug-in hybrid electric vehicle control strategy: comparison between EV and charge-depleting options," presented at the SAE World Congr. Exh., Detroit, MI, 2008, Paper SAE 2008-01-0640.
- [25] C. C. Lin, H. Peng, and J. W. Grizzle, "A stochastic control strategy for hybrid electric vehicles," in *Proc. Amer. Control Conf.*, Boston, MA, Jun. 30–Jul. 2, 2004, pp. 4710–4715.
- [26] E. D. Tate, Jr, J. W. Grizzle, and H. Peng, "Shortest path stochastic control for hybrid electric vehicles," *Int. J. Robust Nonl. Control*, vol. 18, no. 14, pp. 1409–1429, 2008.
- [27] P. Kulshrestha, L. Wang, M.-Y. Chow, and S. Lukic, "Intelligent energy management system simulator for PHEVs at municipal parking deck in a smart grid environment," in *Proc. IEEE PES*, Jul. 26–30, 2009, pp. 1–6.
- [28] A. R. Salisa, N. Zhang, and J. G. Zhu, "A comparative analysis of fuel economy and emissions between a conventional HEV and the UTS PHEV," *IEEE Trans. Veh. Technol.*, vol. 60, no. 1, pp. 44–54, Jan. 2011.
- [29] M. D. Galus, R. La Fauci, and G. Andersson, "Investigating PHEV wind balancing capabilities using heuristics and model predictive control," in *Proc. IEEE Power Energy Soc. Gen. Meeting*, Jul. 25–29, 2010, pp. 1–8.
- [30] P. Pisu and G. Rizzoni, "A comparative study of supervisory control strategies for hybrid electric vehicles," *IEEE Trans. Control Syst. Technol.*, vol. 15, no. 3, pp. 506–518, May 2007.

- [31] P. Tulpule, V. Marano, and G. Rizzoni, "Effects of different PHEV control strategies on vehicle performance," in *Proc. ACC*, Jun. 10–12, 2009, pp. 3950–3955.
- [32] Q. Gong, Y. Li, and Z.-R. Peng, "Trip-based optimal power management of plug-in hybrid electric vehicles," *IEEE Trans. Veh. Technol.*, vol. 57, no. 6, pp. 3393–3401, Nov. 2008.
- [33] Q. Gong, Y. Li, and Z.-R. Peng, "Trip-based optimal power management of plug-in hybrid electric vehicle with advanced traffic modeling," in *Proc. SAE World Congr. Exh.*, Detroit, MI, 2008.
- [34] X. Lin, H. Banvait, S. Anwar, and Y. Chen, "Optimal energy management for a plug-in hybrid electric vehicle: Real-time controller," in *Proc. ACC*, Jun. 30, –Jul. 2, 2010, pp. 5037–5042.
- [35] Y. Bin, Y. Li, Q. Gong, and Z.-R. Peng, "Multi-information integrated trip specific optimal power management for plug-in hybrid electric vehicles," in *Proc. ACC*, Jun. 10–12, 2009, pp. 4607–4612.
- [36] Q. Gong, Y. Li, and Z. Peng, "Power management of plug-in hybrid electric vehicles using neural network based trip modeling," in *Proc. ACC*, Jun. 10–12, 2009, pp. 4601–4606.
- [37] M. Abdul-Hak and N. Al-Holou, "ITS based predictive intelligent battery management system for plug-in hybrid and electric vehicles," in *Proc. IEEE VPPC*, Sep. 7–10, 2009, pp. 138–144.
- [38] C. Zhang and A. Vahid, "Real-time optimal control of plug-in hybrid vehicles with trip preview," in *Proc. ACC*, Jun. 30–Jul. 2, 2010, pp. 6917–6922.
- [39] B. Zhang, M. Zhang, and C. Mi, "Charge depleting control strategies and fuel optimization of blended-mode plug-in hybrid electric vehicles," *IEEE Trans. Veh. Technol.*, vol. 60, no. 4, pp. 1516–1525, May 2011.



Mengyang Zhang (M'08) received the M.S. degree in physics from West Virginia University, Morgantown, in 1993.

He is currently a Senior Technical Specialist with the Chrysler Group LLC, Auburn Hills, MI. His technical areas include powertrain controls and calibrations for Chrysler hybrid electric vehicle programs and advanced vehicle electrification technologies. He has over 18 years experience in research and development of automotive products, including advanced powertrain, electric drive systems, and chassis

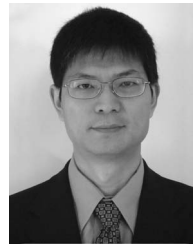
systems.

Mr. Zhang taught a short course on "Fundamentals of HEV Powertrains" for IEEE Vehicular Technology Society in 2010.



Yan Yang received the B.S.E.E. and M.S.C.E. degrees from Xi'an Jiaotong University, Xi'an, China, and the M.S.E.E. degree from the University of Michigan-Dearborn.

She is currently with Cummins, Inc., Columbus, IN. Her research interests are in the optimization of plug-in hybrid electric vehicles.



Chunting Chris Mi (S'00–A'01–M'01–SM'03–F'12) received the B.S.E.E. and M.S.E.E. degrees in electrical engineering from Northwestern Polytechnical University, Xi'an, China, and the Ph.D. degree in electrical engineering from the University of Toronto, Toronto, ON, Canada.

He was previously an Electrical Engineer with General Electric Canada Inc., Peterborough, ON. He is an Associate Professor of electrical and computer engineering and the Director of the newly established DOE GATE Center for Electric Drive Transporta-

tion, University of Michigan-Dearborn. He has conducted extensive research and published more than 100 articles. His research interests include electric drives, power electronics, electric machines, renewable energy systems, and electrical and hybrid vehicles.

Dr. Mi has received the "Distinguished Teaching Award" and "Distinguished Research Award" from the University of Michigan-Dearborn. He also received the 2007 IEEE Region 4 "Outstanding Engineer Award," the "IEEE Southeastern Michigan Section Outstanding Professional Award," and the "SAE Environmental Excellence in Transportation (E2T) Award." He was the Chair (2008–2009) and Vice Chair (2006–2007) of the IEEE Southeastern Michigan Section. He was the General Chair of the Fifth IEEE Vehicle Power and Propulsion Conference, held in Dearborn, on September 6–11, 2009. He is an Associate Editor of the IEEE TRANSACTIONS ON VEHICULAR TECHNOLOGY and the IEEE TRANSACTIONS ON POWER ELECTRONICS—LETTERS, Senior Editor of the IEEE VEHICULAR TECHNOLOGY MAGAZINE, Guest Editor of the *International Journal of Power Electronics*, Editorial Board member of the *International Journal of Electric and Hybrid Vehicles*, Editorial Board member of the *IET Electrical Systems in Transportation*, and was Associate Editor of the *Journal of Circuits, Systems, and Computers* from 2007 to 2009.